

# MIXED CONVECTION FLOW IN A RECTANGULAR VENTILATED CAVITY WITH A HEAT CONDUCTING SOLID CIRCULAR CYLINDER AT THE CENTER

Md. Mustafizur Rahman\*, Md. Elias and Md.A. Alim

Department of Mathematics, Bangladesh University of Engineering and Technology  
Dhaka-1000, Bangladesh  
mmustafizurrahman@math.buet.ac.bd - melias@math.buet.ac.bd - maalim@math.buet.ac.bd

\*Corresponding Author

(Received: December 3, 2008 – Accepted in Revised Form: October 5, 2009)

**Abstract** A numerical investigation has been carried out for mixed convection flow in a rectangular ventilated cavity with a heat conducting solid circular cylinder at the center. Forced convection flow conditions were imposed by providing an inlet at the bottom of the left wall and an outlet vent at the top to the other sidewall. In this paper, the effect of cavity aspect ratio as well as the mixed convection parameter on the flow and heat transfer characteristics were analyzed. Finite element method was used to carry out the investigation. Computations were done for mixed convective flow with the Richardson number  $Ri$  ranging from 0.0 to 5.0, cavity aspect ratio from 0.5 to 2.0 and Reynolds number,  $Re$  of 100. The basic nature of the resulting interaction between the forced external air stream and the buoyancy-driven flow by the heat source was explained by the patterns of the streamlines and isotherms. The computational results indicated that the flow and thermal fields as well as average Nusselt number at the hot wall, average temperature of the fluid and the temperature at the cylinder center strongly depended on the cavity aspect ratio and mixed convection parameter  $Ri$ .

**Keywords** Mixed Convection, Finite Element Method, Richardson Number, Rectangular Cavity, Circular Cylinder

**چکیده** یک مطالعه عددی بر روی جریان جابه جایی (همرفت) مخلوط در یک حفره تهویه شده مستطیلی شکل با یک استوانه جامد رسانای حرارتی در مرکز انجام شد. با ایجاد یک ورودی در کف دیواره سمت چپ و یک دریچه خروجی در بالای دیواره جانبی شرایط جریانی اجباری برقرار شد. در این مقاله، تاثیر نسبت ابعاد حفره و نیز پارامتر (انتقال حرارت به روش) جابه جایی مخلوط بر مشخصات جریان و انتقال حرارت مورد تحلیل قرار گرفت. روش المنت محدود برای انجام این تحقیق مورد استفاده قرار گرفت. محاسبات برای جریان جابه جایی مخلوط با عدد Richardson  $Ri$ ، در محدوده صفر تا ۵/۰، نسبت ابعاد حفره ۰/۵ تا ۲/۰ و عدد Reynolds  $Re$ ، معادل ۱۰۰ انجام شد. ماهیت اصلی برهم کنش حاصل بین جریان هوای اجباری خارجی و جریان شناوری حاصل از منبع گرما توسط الگوهای خطوط جریان و همدمها شرح داده شد. نتایج محاسباتی نشان داد که نواحی جریانی و حرارتی و همچنین عدد Nusselt در دیواره داغ، دمای متوسط جریان و دما در مرکز استوانه شدیداً به نسبت ابعاد حفره و پارامتر جابه جایی مخلوط  $Ri$  بستگی داشت.

## 1. INTRODUCTION

Flow and heat transfer due to the combined effect of free and forced convection are often encountered in engineering system, for example cooling of electronic devices, furnaces, lubrication technologies, chemical processing equipment, drying technologies, etc. [1,2]. Analysis of the above phenomena incorporating a solid heat conducting obstruction extends its usability to various other practical situations. Particularly a

conductive material in an inert atmosphere inside a furnace with a constant flow of gas from outside constitutes a practical application of the present simulation. Many authors have recently studied heat transfer in enclosures with partitions, which influence the convection flow phenomenon.

Omri, et al [1] considered mixed convection in an air-cooled cavity with differentially heated vertical isothermal sidewalls having inlet and outlet ports by a control volume finite element method. They investigated two different placement

configurations of the inlet and outlet ports on the sidewalls. Best configuration was selected by analyzing the cooling effectiveness of the cavity, which suggested that injecting the air through the cold wall was more effective in heat removal and placing inlet near the bottom and outlet near the top produce effective cooling. Later on, Singh, et al [2] extended their works by considering six placement configurations of the inlet and exit ports of a differentially heated rectangular enclosure whereas the previous work was limited to only two different configurations of inlet and outlet port. At the same time, a numerical analysis of laminar mixed convection in an open cavity with a heated wall bounded by a horizontally insulated plate was presented by Manc, et al [3], where three heating modes were considered: assisting flow, opposing flow and heating from below. Results were reported for Richardson number from 0.1 to 100, Reynolds numbers from 100 to 1000 and aspect ratio in the range 0.1–1.5. They showed that the maximum temperature values decreased as the Reynolds and the Richardson numbers increased. The effect of the ratio of channel height to the cavity height was found to play a significant role in streamline and isotherm patterns for different heating configurations. The investigation also indicated that opposing forced flow configuration had the highest thermal performance, in terms of both maximum temperature and average Nusselt number. Later, similar problem for the case of assisting forced flow configuration was tested experimentally by Manca, et al [4] and based on the flow visualization results, they pointed out that for  $Re = 1000$  there were two nearly distinct fluid motions: a parallel forced flow in the channel and a recirculation flow inside the cavity and for  $Re = 100$  the effect of a stronger buoyancy determined a penetration of thermal plume from the heated plate wall into the upper channel. Recently Rahman, et al [5] studied numerically the opposing mixed convection in a vented enclosure. They found that with the increase of Reynolds and Richardson numbers the convective heat transfer was predominant over the conduction heat transfer and the rate of heat transfer from the heated wall was significantly depended on the position of the inlet port. Very recently Manca, et al [6] experimentally analyzed opposing flow in mixed convection in a channel with an open cavity below.

However, many authors have studied heat transfer in enclosures with heat-conducting body obstruction thereby influencing the convective flow phenomenon. Shuja, et al [7] investigated the effect of outlet port locations and aspect ratio of the heat generating body on the heat transfer characteristics and irreversibility generation in a square cavity. They found that the overall normalized Nusselt number as well as irreversibility was strongly affected by both of the location of outlet port and aspect ratios. Papanicolaou, et al [8] studied mixed convection from an isolated heat sources in a rectangular enclosure. Later on, Papanicolaou, et al [9] performed computations on mixed convection from a localized heat source in a cavity with conducting walls and two openings for application of electronic cooling equipment. Hsu, et al [10] numerically investigated mixed convection in a partially divided rectangular enclosure. They considered the divider as a baffle inside the enclosure with two different orientations and indicated that the average Nusselt number and the dimensionless surface temperature were dependent on the locations and height of the baffle. Natural convection in a horizontal layer of fluid with a periodic array of square cylinder in the interior were conducted by Ha, et al [11], in which they concluded that the transition of the flow from quasi-steady up to unsteady convection depended on the presence of bodies and aspect ratio effect of the cell. However, in the previous literature the body was considered as a rigid wall but internal heat transfer was not calculated. Few numerical studies, taking into account heat transfer in the interior of the body, have been conducted over the past couple of decades. One of the systematic numerical investigations of this problem was conducted by House, et al [12], who considered natural convection in a vertical square cavity with heat conducting body, placed on the center in order to understand the effect of the heat conducting body on the heat transfer process in the cavity. They showed that for given  $Ra$  and  $Pr$ , an existence of conducting body with thermal conductivity ratio less than unity led to heat transfer enhancement.

The problem of mixed convection in a rectangular ventilated cavity with a heat conducting solid circular cylinder at the center has not been studied in details earlier. The objective of the

present study is to gain some insight into fluid motion and heat transfer phenomena in case of a rectangular ventilated cavity with a heat conducting solid circular cylinder at the center. In the present case, we have considered a rectangular ventilated cavity with a heat conducting solid circular cylinder at the center, where  $Re$  has been kept at 100 while the  $Gr$  has been varied and keeping the  $Pr = 0.71$ . The aspect ratio (height/width) of the cavity was considered as 0.5, 1.0, 1.5 and 2.0. The results are shown in terms of parametric presentations of streamlines and isotherms plots in the cavity. Also, the effect of mixed convection parameter,  $Ri$  and cavity aspect ratio on the heat transfer process are analyzed and the results are presented in terms of the average Nusselt number at the heated surface, average temperature of the fluid in the cavity and the temperature at the cylinder center.

## 2. MODEL DESCRIPTION

Details of the geometry of the configuration are shown in Figure 1. The model considered here is a rectangular ventilated cavity with a uniform constant temperature  $T_h$ , applied on the right vertical wall. The cavity has dimensions of  $L \times H$ . The other sidewalls including top and bottom of the cavity are assumed to be adiabatic. The inflow

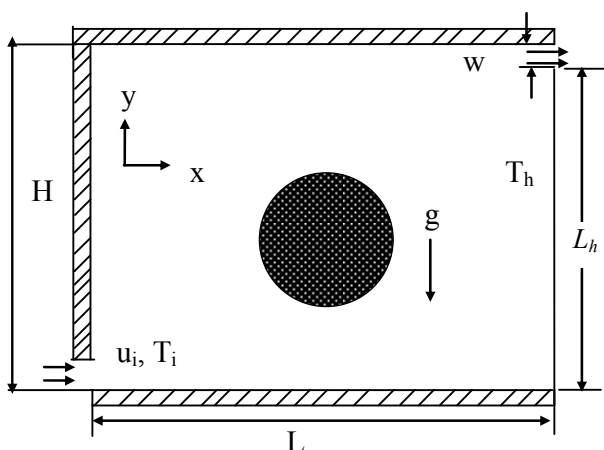


**Figure 1.** Schematic of the problem with the domain and boundary conditions.

opening located on the left vertical wall is arranged as shown in the Figure 1. The outflow opening of the cavity is fixed at the top of the opposite heated wall and the size of the inlet port is the same as the outlet port which is equal to  $w = 0.1H$ . It is assumed that the incoming flow is at a uniform velocity,  $u_i$  at the ambient temperature,  $T_i$  and the outgoing flow is assumed to have zero diffusion flux for all dependent variables i.e. convective boundary conditions (CBC). The cylinder, having a diameter of  $H/5$ , is placed at the center of the rectangular cavity and no slip boundary conditions are assumed on the cylinder surface and all solid boundaries.

## 3. MATHEMATICAL FORMULATIONS

**3.1. Governing Equations** Mixed convection is governed by the partial differential equations expressing conservation of mass, momentum and energy. The present flow is considered steady, laminar, incompressible and two-dimensional. The viscous dissipation term in the energy equation is neglected. The physical properties of the fluid in the flow model are assumed to be constant, except the density variations causing a body force term in the momentum equation. The Boussinesq approximation is invoked for the fluid properties to relate density changes to temperature changes, and to couple in this way the temperature field to the flow field. The governing equations for steady mixed convection flow can be expressed in the dimensionless form as:

$$\frac{\partial U}{\partial X} + \frac{\partial V}{\partial Y} = 0 \quad (1)$$

$$U \frac{\partial U}{\partial X} + V \frac{\partial U}{\partial Y} = -\frac{\partial P}{\partial X} + \frac{1}{Re} \left( \frac{\partial^2 U}{\partial X^2} + \frac{\partial^2 U}{\partial Y^2} \right) \quad (2)$$

$$U \frac{\partial V}{\partial X} + V \frac{\partial V}{\partial Y} = -\frac{\partial P}{\partial Y} + \frac{1}{Re} \left( \frac{\partial^2 V}{\partial X^2} + \frac{\partial^2 V}{\partial Y^2} \right) + Ri\Theta \quad (3)$$

$$U \frac{\partial \Theta}{\partial X} + V \frac{\partial \Theta}{\partial Y} = \frac{1}{Re Pr} \left( \frac{\partial^2 \Theta}{\partial X^2} + \frac{\partial^2 \Theta}{\partial Y^2} \right) \quad (4)$$

For heat conducting cylinder, the energy equation is expressed as:

$$\frac{\partial^2 \Theta_s}{\partial X^2} + \frac{\partial^2 \Theta_s}{\partial Y^2} = 0 \quad (5)$$

Where X and Y are the coordinates varying along horizontal and vertical directions respectively, U and V are the velocity components in the X and Y directions, respectively,  $\Theta$  is the dimensionless temperature and P is the dimensionless pressure. The non-dimensional parameters seen in the above equations are the Reynolds number Re, Richardson number Ri, Prandtl number Pr and solid fluid thermal conductivity ratio K which are defined as:

$$Re = \frac{u_i H}{\nu}, Ri = \frac{g\beta(T - T_i)H}{u_i^2}, Pr = \frac{\nu}{\alpha} \text{ and } K = \frac{k_s}{k}$$

The dimensionless parameters in the equations above are defined as follows:

$$X = \frac{x}{H}, Y = \frac{y}{H}, U = \frac{u}{u_i}, V = \frac{v}{u_i},$$

$$P = \frac{P}{\rho u_i^2}, \Theta = \frac{(T - T_i)}{(T_h - T_i)}, \Theta_s = \frac{(T_s - T_i)}{(T_h - T_i)}$$

Where  $\rho$ ,  $\beta$ ,  $\nu$ ,  $\alpha$  and  $g$  are the fluid density, coefficient of volumetric expansion, kinematic viscosity, thermal diffusivity, and gravitational acceleration, respectively.

The appropriate dimensionless form of the boundary conditions (as shown in Figure 1) used to solve Equations 1-5 inside the cavity are given as follow:

At the inlet:  $U = 1, V = 0, \Theta = 0$

At the outlet:  $P = 0$

At all solid boundaries:  $U = 0, V = 0$

At the heated right vertical wall:  $\Theta = 1$

At the left, top and bottom walls in the cavity:

$$\left. \frac{\partial \Theta}{\partial X} \right|_{X=0} = \left. \frac{\partial \Theta}{\partial Y} \right|_{Y=1,0} = 0$$

At the solid-fluid vertical interfaces of the block:

$$\left( \frac{\partial \Theta}{\partial X} \right)_{fluid} = K \left( \frac{\partial \Theta_s}{\partial X} \right)_{solid}$$

At the solid-fluid horizontal interfaces of the block:

$$\left( \frac{\partial \Theta}{\partial Y} \right)_{fluid} = K \left( \frac{\partial \Theta_s}{\partial Y} \right)_{solid}$$

The average Nusselt number (Nu) at the hot wall is

$$\text{defined as: } Nu = \frac{1}{L_h} \int_0^{L_h} \left. \frac{\partial \Theta}{\partial X} \right|_{X=1} dY$$

and the bulk average temperature in the cavity is

$$\text{defined as: } \Theta_{av} = \frac{1}{\bar{V}} \int \Theta d\bar{V}$$

Where  $L_h$  is the length of the hot wall and  $\bar{V}$  is the cavity volume.

**3.2. Computational Procedure** The numerical procedure used in this work is based on the Galerkin weighted residual method of finite element formulation. The application of this technique is well described by Taylor, et al [13] and Dechaumphai [14]. In this method, the solution domain is discretized into finite element meshes, which are composed of non-uniform triangular elements. Then the nonlinear governing partial differential equations (i.e., mass, momentum and energy equations) are transferred into a system of integral equations by applying Galerkin weighted residual method. The integration involved in each term of these equations is performed using Gauss quadrature. The nonlinear algebraic equations so obtained are modified by imposition of boundary conditions. These modified nonlinear equations are transferred into linear algebraic equations using Newton's method. Finally, using Triangular Factorization method these linear equations are solved.

**3.3. Grid Sensitivity Check** Geometry studied in this paper is an obstructed ventilated cavity; therefore several grid size sensitivity tests were conducted in this geometry to determine the sufficiency of the mesh scheme and to ensure that the solutions are grid independent. This is obtained when numerical results of the average Nusselt number Nu, average temperature  $\Theta_{av}$  and solution time become grid size independent, although the refinement of the mesh grid is continued. For the cavity with AR = 1.0, five different non-uniform grids with the following number of nodes and elements were considered for

the grid refinement tests:

- G<sub>1</sub>25555 nodes, 3976 elements
- G<sub>2</sub>30619 nodes, 4798 elements
- G<sub>3</sub>38973 nodes, 6158 elements
- G<sub>4</sub>39870 nodes, 6278 elements and
- G<sub>5</sub>48945 nodes, 7724 elements

as shown in Table 1. Figure 2 shows the average Nusselt number profiles at the heated surface for the aforementioned five different grids. From these values 39870 nodes and 6278 elements have been chosen for the cavity with AR = 1.0. Similarly, grid sensitivity test has been done for the cavity with AR = 0.5, 1.5 and 2.0 (data not shown).

However, the present numerical technique will discretize the computational domain into unstructured triangles by Delaunay Triangular method. The Delaunay triangulation is a geometric structure that has enjoyed great popularity in mesh generation since the mesh generation was in its infancy. The mesh mode for the present numerical computation is shown in Figure 3.

**3.4. Code Validation** The present code was extensively validated based on the problem of House, et al [12]. Some of the results obtained from current study are compared with those reported by House, et al [12] for Ra = 0.0, 10<sup>5</sup> and two values of K = 0.2 and 5.0. The physical problem studied by House, et al [12] was a vertical

square enclosure with sides of length L. The vertical walls were isothermal and differentially heated, where as the bottom and top walls were adiabatic. A square heat conducting body with side length of L/2 was placed at the center of the enclosure. For the same parameters used by House, et al [12]; the average Nusselt number (at the hot wall) comparison is shown in Table 2. The present results have an excellent agreement with the results obtained by House, et al [12].

## 4. RESULTS AND DISCUSSIONS

Two-dimensional mixed convection is studied for a laminar flow in an air-cooled rectangular cavity containing a heat conducting solid cylinder at the center with a Prandtl number of 0.71. The controlling parameter, for the problem is Richardson number, Ri. The Reynolds number, Re, and solid fluid thermal conductivity ratio, K, are kept fixed at 100 and 5.0, respectively. The range of Richardson number used for the simulations is  $0.0 \leq Ri \leq 5.0$  and it is obtained by varying the Grashof number only. The considered aspect ratio is in the range of 0.5 to 2.0.

### 4.1. Flow and Thermal Fields Characteristics

The combined forced and buoyancy driven flow and temperature fields inside a ventilated cavity, with a heat conducting solid circular cylinder at the

TABLE 1. Grid Sensitivity Check at Re = 100, Ri = 1.0, AR = 1.0 and Pr = 0.71.

| Elements (Nodes) | 3976 (25555) | 4798 (30619) | 6158 (38973) | 6278 (39870) | 7724 (48945) |
|------------------|--------------|--------------|--------------|--------------|--------------|
| Nu               | 4.8463       | 4.8478       | 4.8480       | 4.8489       | 4.8528       |
| $\Theta_{av}$    | 0.1905       | 0.1905       | 0.1905       | 0.1905       | 0.1905       |
| Time(s)          | 385.219      | 493.235      | 682.985      | 698.703      | 927.359      |

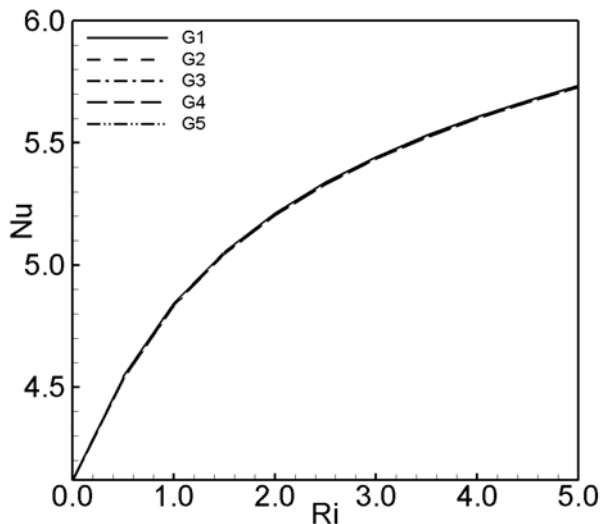


Figure 2. Grid Sensitivity Test for AR = 1.0.

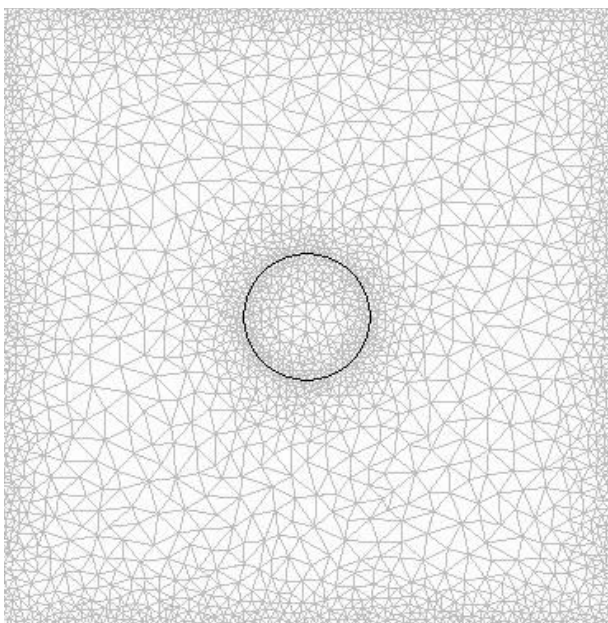


Figure 3. Grid used for numerical simulations for AR = 1.0.

center, for different cavity configurations have been illustrated by streamlines and isotherms in Figures 4-6, for Richardson numbers of 0.0, 1.0 and 5.0, respectively. Figure 4 shows the dynamics and thermal field for the  $Ri = 0.0$  in terms of streamlines and isotherm surfaces for different AR values. At  $Ri = 0.0$ , for the lower AR values,

forced convection dominates the major flow from the inlet to the outlet without much penetrating into the cavity. The presence of a small rotating cell in the clockwise direction located near the opposite insulated wall starting from the inflow is observed. On the other hand, a very small rotating cell is also seen in the right bottom corner in the cavity because, entering cold fluids cannot intimately mix with the hot fluids. From these figures it has been clearly seen that the size of the rotating cell increased with AR. The corresponding isotherm plots are presented in Figures 4b (i-iv). As expected, the thermal boundary decreases in thickness as AR increases. This is reflected by the dense clustering of the isotherms close to the hot wall as AR is increased.

Figure 5 shows the streamlines and isotherms for  $Ri = 1.0$  and different cavity configuration. It is seen from Figure 5a (i-iv) that the natural convection effect exists but remains relatively weak at the low  $AR = 0.5$ , since the open lines characterizing the imposed flow are still dominant. On the other hand, for the higher values of AR it is clearly seen that the recirculating cell near the left wall gradually increases with the increase of AR and another recirculating cell is developed just in the front of the outlet port, above the open lines. The corresponding isotherm plots for the above cases are presented in Figures 5b (i-iv). The thermal boundary layer decreases in thickness gradually as the AR increases.

The effect of the cavity aspect ratio on the flow structure and temperature distribution inside the cavity is illustrated in Figure 6 (i-iv) for  $Ri = 5.0$  and four selected values of AR. For  $Ri = 5.0$ , it has been seen that the flow pattern is changed drastically from a small circulating cell to a large circulating cell and thereby squeezes the induced flow path due to the supremacy of natural convection in the cavity. On the other hand, large temperature gradients close to the hot wall and stratified temperature distribution in the rest of the cavity are observed for  $Ri = 5$ .

**4.2. Heat Transfer Characteristics** Representative results on the variation of the local Nusselt number on the heated surface of the cavity for different  $Ri$  and a particular AR are shown in the Figure 7. These figures show qualitatively similar features as seen in Figures 7a-d. Moreover, the effect of

**TABLE 2. Comparison of Average Nusselt Number with House, et al [12].**

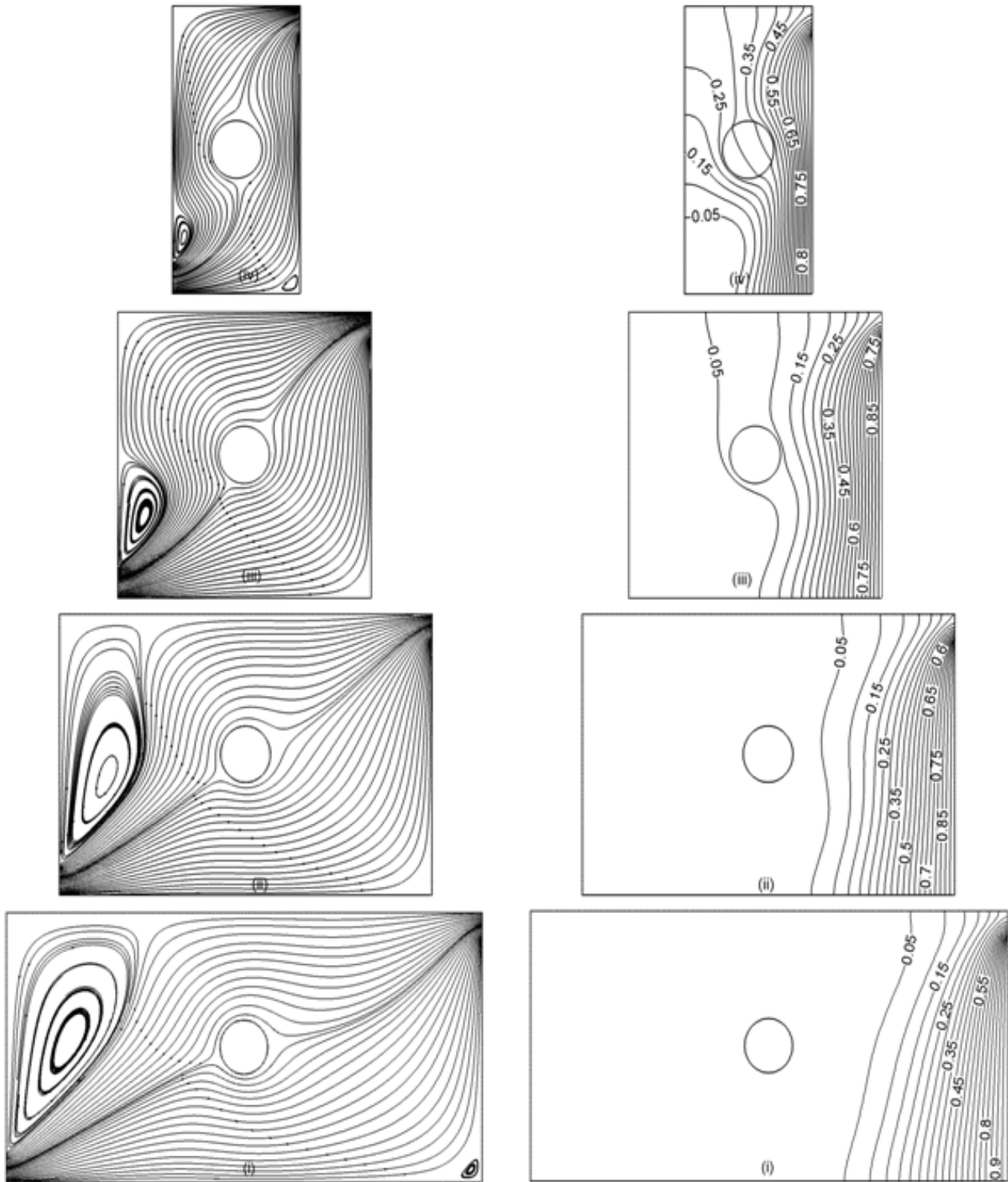
| Ra     | K   | Nu            |                   |
|--------|-----|---------------|-------------------|
|        |     | Present Study | House, et al [12] |
| 0      | 0.2 | 0.7071        | 0.7063            |
| 0      | 1.0 | 1.0000        | 1.0000            |
| 0      | 5.0 | 1.4142        | 1.4125            |
| $10^5$ | 0.2 | 4.6237        | 4.6239            |
| $10^5$ | 1.0 | 4.5037        | 4.5061            |
| $10^5$ | 5.0 | 4.3190        | 4.3249            |

Richardson number on the average Nusselt number at the hot wall, average temperature of the fluid in the cavity, dimensionless temperature at the cylinder center for values of cavity aspect ratio is shown in the Figure 8. As Ri increases, average Nusselt number increases sharply for all values of AR. Average Nusselt number (Nu) is higher for the lower values of AR. On the other hand, the average temperature of the fluid in the cavity and temperature at the cylinder center increases gradually with increasing Ri. The average temperature of the fluid in the cavity and temperature at the cylinder center are lower for the higher values of AR.

## 5. CONCLUSION

Steady mixed convection heat transfer in a

rectangular ventilated cavity operating under laminar regime has been numerically investigated. The investigation was carried out for a number of relevant dimensionless groups, namely the Reynolds number, Richardson number and the cavity aspect ratio. A total of four cavity configurations have been considered. The study encompasses a constant value of Reynolds number (Re) at 100 and a range of Richardson number (Ri) from 0.0 to 5.0, representing dominating forced convection through mixed convection to dominating natural convection. The results of the study show that the flow structure and temperature distribution are considerably influenced by the mixed convection parameter and the cavity aspect ratio. The average Nusselt number at the heated surface is the highest for the lowest value of AR, but the average temperature of the fluid in the cavity and temperature at the cylinder center are the lowest for the highest value of AR.



Streamlines

Isotherms

(a)

(b)

**Figure 4.** (a) Streamlines (left) and (b) Isotherms (right) for (i)  $AR = 2.0$ ,  
(ii)  $AR = 1.5$ , (iii)  $AR = 1.0$  and (iv)  $AR = 0.5$  at  $Ri = 0.0$ .



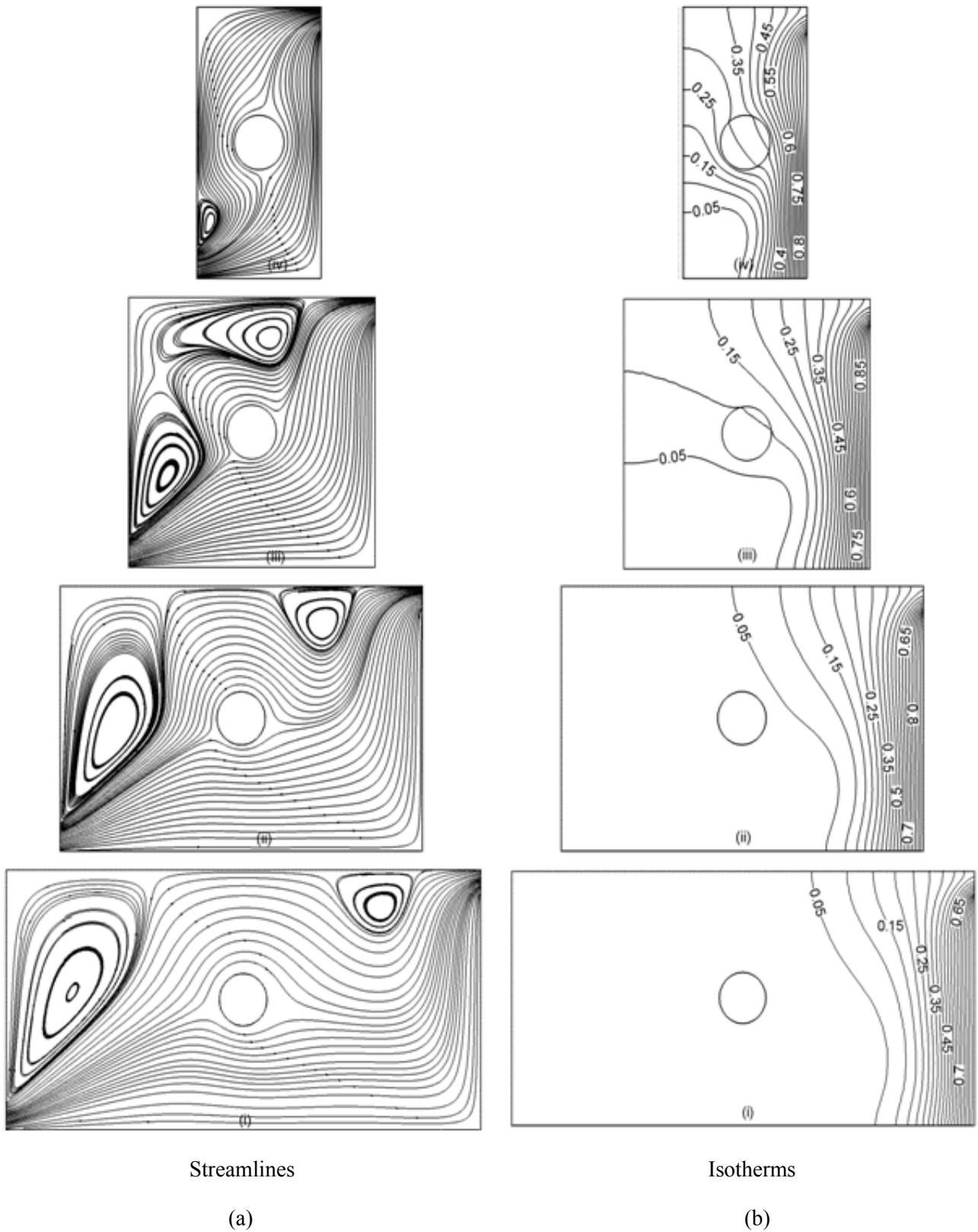
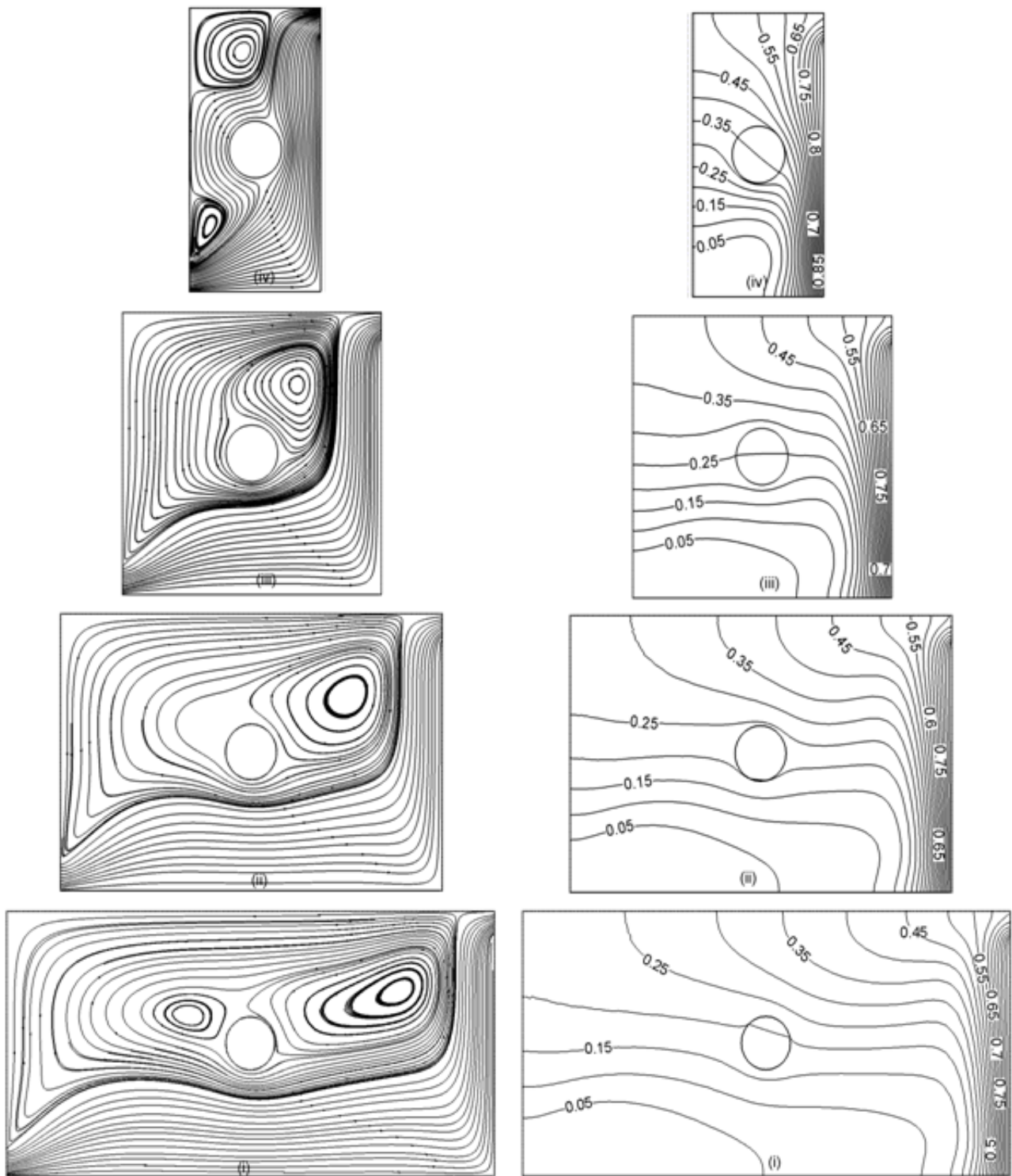


**Figure 5.** (a) Streamlines (left) and (b) Isotherms (right) for (i) AR = 2.0, (ii) AR = 1.5, (iii) AR = 1.0 and (iv) AR = 0.5 at Ri = 1.0.



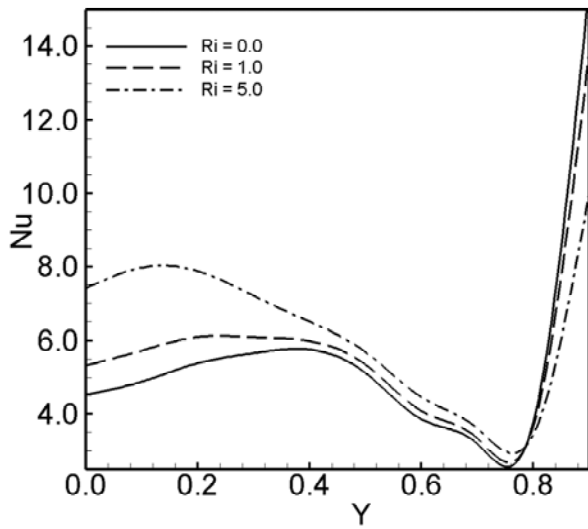
Streamlines

Isotherms

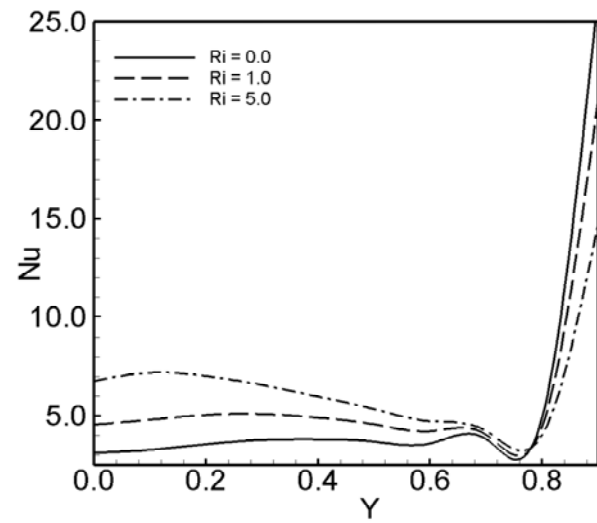
(a)

(b)

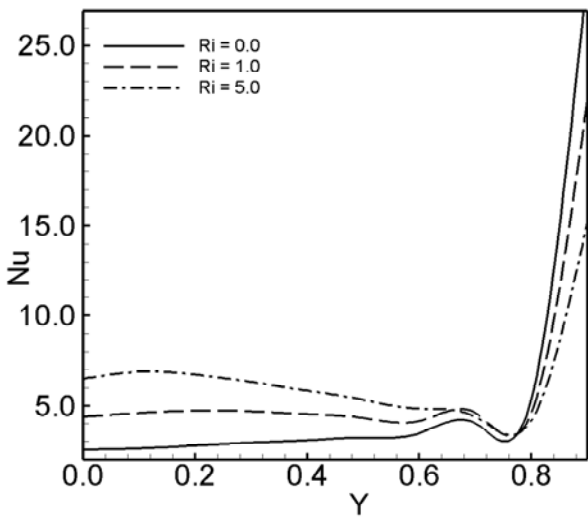
**Figure 6.** (a) Streamlines (left) and (b) Isotherms (right) for (i) AR = 2.0, (ii) AR = 1.5, (iii) AR = 1.0 and (iv) AR = 0.5 at Ri = 5.0.



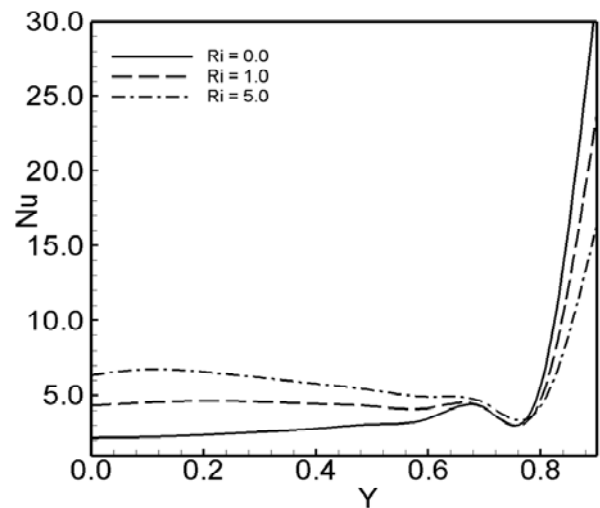
(a)



(b)



(c)



(d)

**Figure 7.** Local Nusselt number at the hot surface for different Ri at (a) AR = 0.5 (b) AR = 1.0, (c) AR = 1.5 and (d) AR = 2.0.

## 6. NOMENCLATURE

|      |  |
|------|--|
| $AR$ | cavity aspect ratio                                      |
| $g$  | gravitational acceleration ( $ms^{-2}$ )                 |
| $Gr$ | Grashof number   |
| $h$  | convective heat transfer coefficient ( $Wm^{-2}K^{-1}$ ) |
| $H$  | height of the cavity ( $m$ )                             |
| $w$  | height of the inflow and outflow openings ( $m$ )        |
| $k$  | thermal conductivity of the fluid ( $Wm^{-1}K^{-1}$ )    |

|       |   |
|-------|---|
| $k_s$ | thermal conductivity of the solid square cylinder ( $Wm^{-1}K^{-1}$ ) |
| $K$   | solid to fluid thermal conductivity ratio                             |
| $L$   | length of the cavity ( $m$ )  |
| $L_s$ | length of the heated wall   |
| $Nu$  | average Nusselt number  |
| $N$   | non-dimensional distance  |
| $p$   | pressure ( $Nm^{-2}$ )  |
| $P$   | non-dimensional pressure  |

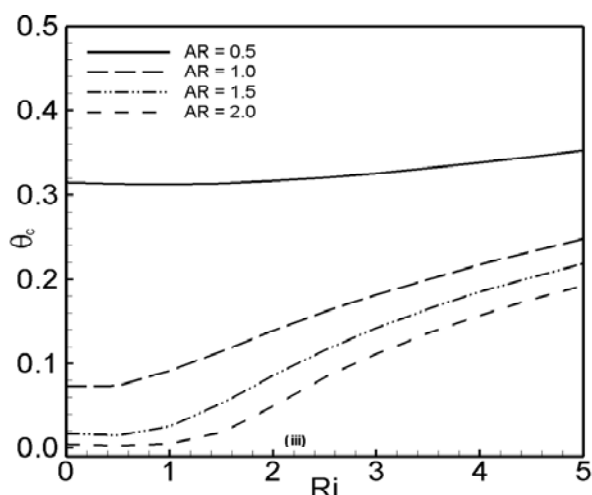
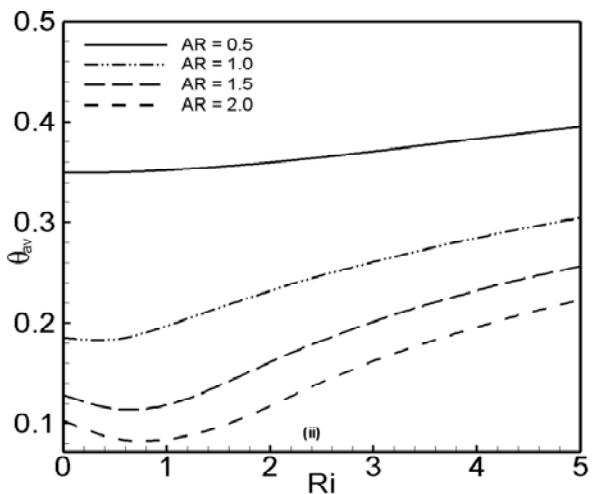
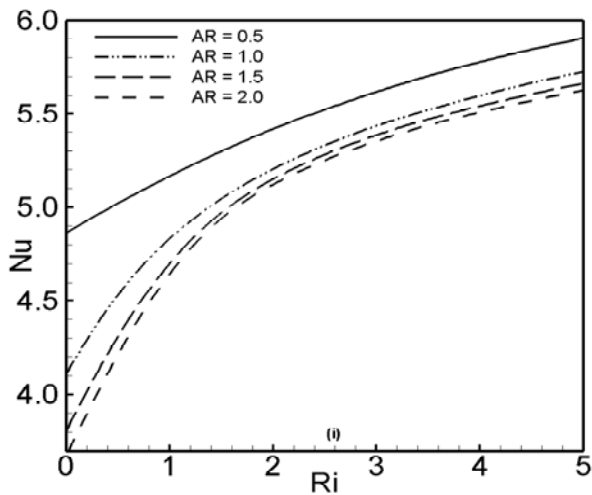


**Figure 8.** Effect of cavity aspect ratio on (i) average Nusselt number, (ii) average temperature and (iii) temperature at the cylinder center for different  $Ri$ .

|           |                                       |
|-----------|---------------------------------------|
| $Pr$      | Prandtl number                        |
| $Ra$      | Rayleigh number                       |
| $Re$      | Reynolds number                       |
| $Ri$      | Richardson number                     |
| $T$       | temperature (K)                       |
| $\Theta$  | non-dimensional temperature           |
| $u, v$    | velocity components ( $ms^{-1}$ )     |
| $U, V$    | non-dimensional velocity components   |
| $\bar{V}$ | cavity volume ( $m^3$ )               |
| $x, y$    | cartesian coordinates (m)             |
| $X, Y$    | non-dimensional cartesian coordinates |

### Greek Symbols

|          |  |
|----------|--|
| $\alpha$ | thermal diffusivity ( $m^2s^{-1}$ )              |
| $\beta$  | thermal expansion coefficient ( $K^{-1}$ )       |
| $\rho$   | density of the fluid ( $kgm^{-3}$ )              |
| $\nu$    | kinematic viscosity of the fluid ( $m^2s^{-1}$ ) |

### Subscripts

|      |                |
|------|----------------|
| $av$ | average        |
| $s$  | heated surface |
| $i$  | inlet state    |

## 7. ACKNOWLEDGEMENTS

The authors wish to acknowledge Department of Mathematics, Bangladesh University of Engineering and Technology, Dhaka, Bangladesh, for support and technical help throughout this work.

## 8. REFERENCES

1. Omri, A. and Nasrallah, S.B., "Control Volume Finite Element Numerical Simulation of Mixed Convection In An Air-Cooled Cavity", *Numerical Heat Transfer, Part A*, Vol. 36, (1999), 615–637.
2. Singh, S. and Sharif, M.A.R., "Mixed Convection Cooling of a Rectangular Cavity with Inlet and Exit Openings on Differentially Heated Side Walls", *Numerical Heat Transfer, Part A*, Vol. 44, (2003), 233–253.
3. Manca, O., Nardini, S., Khanafer, K. and Vafai, K., "Effect of Heated Wall Position on Mixed Convection in a Channel with an Open Cavity", *Numerical Heat Transfer, Part A*, Vol. 43, (2003), 259–282.
4. Manca, O., Nardini, S. and Vafai, K., "Experimental Investigation of Mixed Convection in a Channel with an

- Open Cavity”, *Experimental Heat Transfer*, Vol. 19, (2006), 53–68.
5. Rahman, M.M., Alim, M.A., Mamun, M.A.H., Chowdhury, M.K. and Islam, A.K.M.S., “Numerical Study of Opposing Mixed Convection in a Vented Enclosure”, *Journal of Engineering and Applied Sciences*, Vol. 2, No. 2, (2007), 25-36.
  6. Manca, O., Nardini, S. and Vafai, K., “Experimental Analysis of Opposing Flow in Mixed Convection in a Channel with an Open Cavity Below”, *Experimental Heat Transfer*, Vol. 21, (2008), 99–114.
  7. Shuja, S.Z., Yilbas, B.S. and Iqbal, M.O., “Mixed Convection in a Square Cavity Due to Heat Generating Rectangular Body Effect of Cavity Exit Port Locations”, *International Journal of Numerical Methods for Heat and Fluid Flow*, Vol. 10, No. 8, (2000), 824–841.
  8. Papanicolaou, E. and Jaluria, Y., “Mixed Convection From an Isolated Heat Source in a Rectangular Enclosure”, *Numerical Heat Transfer*, Part A, Vol. 18, (1990), 427–461.
  9. Papanicolaou, E. and Jaluria, Y., “Mixed Convection from a Localized Heat Source in a Cavity with Conducting Walls: A Numerical Study”, *Numerical Heat Transfer*, Part A, Vol. 23, (1993), 463–484.
  10. Hsu, T.H., Hsu, P.T. and How, S.P., “Mixed Convection in a Partially Divided Rectangular Enclosure”, *Numerical Heat Transfer*, Part A, Vol. 31, (1997), 655-683.
  11. Ha, M.Y., Yoon, H.S, Yoon, K.S., Balachandar, S., Kim, I., Lee, J.R. and Chun, H.H., “Two-Dimensional and Unsteady Natural Convection in a Horizontal Enclosure with a Square Body”, *Numerical Heat Transfer*, Part A, Vol. 41, (2002), 183–210.
  12. House, J.M., Beckermann, C. and Smith, T.F., “Effect of a Centered Conducting Body on Natural Convection Heat Transfer in an Enclosure”, *Numerical Heat Transfer*, Part A, Vol. 18, (1990), 213–225.
  13. Taylor, C. and Hood, P., “A Numerical Solution of the Navier-Stokes Equations using Finite Element Technique”, *Computer And Fluids*, Vol. 1, (1973),73-89.
  14. Dechaumphai, P., “Finite Element Method in Engineering”, 2<sup>nd</sup> Ed., Chulalongkorn University Press, Bangkok, Thailand, (1999).